Journal of the Physical Society of Japan
Vol. 71, No. 1, January, 2002, pp. 15–18

Dynamic and Static Frictions of the System with Two Particles in a Box

Akinori Awazu*

Department of Pure and Applied Sciences,
University of Tokyo, Komaba 3-8-1, Meguro-ku, Tokyo 153-8902

(Received June 27, 2001)

The appearances and the change of the frictional force of a system with two hard spheres in a two-dimensional rectangular box are discussed. With controlling the pressure or the supply of energy from the wall, the solid-like state, the solid-liquid temporal coexistence state, and the liquid-like state are observed. The frictional force and the fluidity of the system are measured under the shear. By varying the shear, a marked change of frictional forces is observed with similar characteristics to those of the static and dynamic frictions of a solid-on-solid system. Moreover, the relationship between the above frictional force and the shear is found to show strong temperature dependency. The hysteresis loop in the friction-velocity relation on granular layers [S. Nasuno *et al.*: Phys. Rev. Lett. **79** (1997) 949] is discussed on the base of these results.

KEYWORDS: static friction, dynamic friction, granular friction
DOI: 10.1143/JPSJ.71.15

The existence of static friction and dynamic friction and the change between them are universal phenomena commonly observed at the surfaces of macro scale objects,[1–12] and are important subjects of fundamental physics. They have been experientially believed to satisfy Coulomb–Amontons's laws: I) The magnitude of the frictional force depends not on the contact area between two objects but on the magnitude of the normal load between them. II) The maximum static friction coefficient is larger than the dynamic one, and the dynamic one is constant, independent of the sliding velocity. The mechanism and characteristic features of frictions and lubrication have been studied using several microscopic models which consist of a large number of atoms.[4] From the microscopic point of view, the change between the above two types of frictions is expected to have a close relationship with the melting and freezing at a surface region. The liquid-solid phase transition in this case is caused by external driving forces such as shear forces, which means that this transition occurs under non-equilibrium states. In numerical simulations of systems containing 10^1–10^4 hard- or soft-core particles, the liquid-solid phase transition with a van der Waals loop was observed.[13–20] Similar phenomena were also observed in the system with two hard spheres in a rectangular box.[21] This system showed not only behavior like a solid-liquid phase transition but also behavior like a glass transition with the appearance of α- and β- like relaxation and the disappearance of the van der Waals loop. In this paper, we discuss the appearance of some types of friction and the change between them through a simple model similar to that introduced in the previous paper,[21] but with a few modifications.

The system under consideration consists of two-dimensional hard sphere particles with unit mass and unit radius which are confined in a two-dimensional rectangular box (Fig. 1). The right-hand wall with unit mass of the box can move in the horizontal direction. The position of the right-hand wall is $X(t)$ ($X(t) > 2$) and the constant force $-f$ is applied to this wall in the horizontal direction. This force corresponds to a normal load in the general treatment of frictions. The left-hand wall is set at the origin of the horizontal axis and is in contact with the energy source. The bottom of the box is set at zero height in the vertical direction, and the position of the top of the box (the box height) is Y ($Y > 4$). All walls are rigid, and interactions between two particles, as well as those between a particle and a wall without an energy source, occur only through hard-core collisions. These collisions are implemented in the following manner: the tangential velocities to the collision plane are preserved, while the normal component of relative velocity Δv_n becomes $-\Delta v_n$. A particle hitting the left-hand wall in contact with the energy source with the velocity $(v_\mathrm{h}, v_\mathrm{v})$ bounces back with the velocity $(V_\mathrm{h}, V_\mathrm{v})$ ($V_\mathrm{h} > 0$). Here, subscripts h and v indicate, respectively, the horizontal and vertical directions. The velocity $(V_\mathrm{h}, V_\mathrm{v})$ is chosen randomly from the probability distributions $P_\mathrm{h}(V_\mathrm{h})$ and $P_\mathrm{v}(V_\mathrm{v})$:[22]

$$P_\mathrm{h}(V_\mathrm{h}) = T^{-1} V_\mathrm{h} \exp\left(-\frac{V_\mathrm{h}^2}{2T}\right) \tag{1}$$

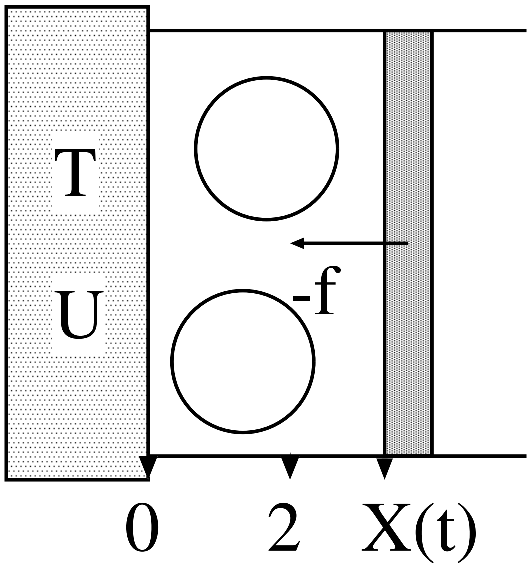

Fig. 1. Illustration of two-particle system in a box with a moving wall (right) and energy sources (left).

*E-mail: awa@complex.c.u-tokyo.ac.jp

$$P_{\mathrm{v}}(V_{\mathrm{v}}) = (2\pi T)^{-\frac{1}{2}} \exp\left(-\frac{(V_{\mathrm{v}} - U)^2}{2T}\right), \tag{2}$$

where T is the temperature of the energy source. (We give the Boltzmann constant as 1.) In the case of $U \neq 0$, asymmetric force works on the system from the energy source in the vertical direction. We consider only the case of $Y > 4$, which means that the two particles can exchange their positions in the horizontal direction. When $X(t) > 4$, these spheres can exchange their positions in the vertical direction. In contrast, these particles cannot exchange their positions in the vertical direction when $X(t) < 4$. In the previous paper, we fixed $X(t) = X$ and defined the state with $X > 4$ as the liquid-like state and that with $X < 4$ as the solid-like state.[21] In this paper, however, because we treat the probability distributions of $X(t)$, we slightly modify the definitions of these states as follows: the solid-like state is defined as the state in which the probability distribution of $X(t)$ has a peak at $X(t) < 4$, and the liquid-like state is defined as the state in which the distribution has a peak at $X(t) > 4$.

Before discussing frictions, we note that transitions between the liquid-like and solid-like states are observed in a small system under equilibrium and non-equilibrium conditions. First, we discuss the case of $U = 0$ that corresponds to the case in which a heat bath is connected to the left-hand wall. Figure 2 shows the probability distribution of the position of the right-hand wall $X(t)$ for some values of f with (a) $Y = 4.5$, (b) $Y = 5.0$, and (c) $Y = 5.5$ at the same temperature T $(= 0.1)$. Independently of Y, each distribution has only one peak at $X(t) < 4$ for large f (solid-like state), or $X(t) > 4$ for small f (liquid-like state). For mid-range f, however, each distribution has two peaks for the case of $Y \leq 5.0$. One at $X(t) < 4$ and the other at $X(t) > 4$ [Fig. 2(a)]. Here, the system passes between the liquid-like and solid-like states. Thus, the transition between the solid-like and liquid-like states appears. This transition is regarded as a trace of the liquid-solid phase transition in a system with an infinite number of particles.[13–20] These two peaks become blunt with the increase of Y, and the probability distribution around $X(t) = 4.0$ becomes almost flat for $Y \sim 5.0$ [Fig. 2(b)]. In contrast, in the case of $Y \leq 5.0$, each distribution always has only one peak for all values of f when $Y > 5.0$ [Fig. 2(c)]. The appearance and the disappearance of such transitions are considered to be strongly related to those of Van der Waals loop observed when the width of the box is fixed.[21] However, the height without a transition is $Y > Y^* \sim 5.0$, which is smaller than the height of the disappearance of the van der Waals loop $Y'^* \sim 6.0$ in our previous paper.[21] Our value Y^* is similar to another critical height $Y'_{\mathrm{c}} \sim 5.0$ found for the previous model, where β- and α- like relaxations appear for $Y' \geq Y'_{\mathrm{c}}$.[21] If we fix f and change the value $\beta = 1/T$, we observe qualitatively the same results as given above.

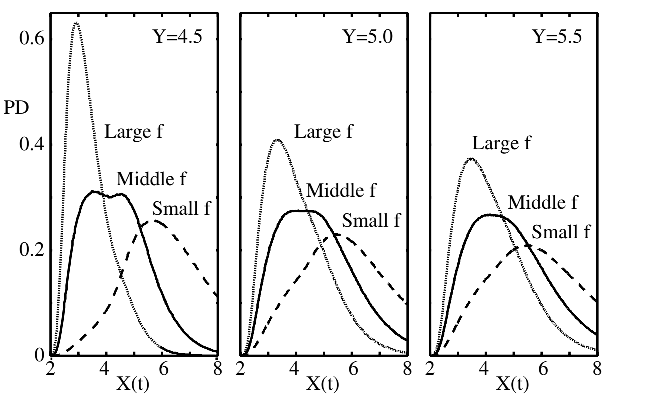

Fig. 2. Probability distribution of the position of the right-hand wall $X(t)$ (PD) for several values of f when (a) $Y = 4.5$ (middle $f = 0.1725$), (b) $Y = 5.0$ (middle $f = 0.1345$), and (c) $Y = 5.5$ (middle $f = 0.1225$) for $T = 0.1$ and $U = 0$.

Next, we discuss the case with $U > 0$. In this case, the system is in a non-equilibrium state because of the asymmetric force acting on particles in the vertical direction by the shear at the left-hand wall. Figure 3 shows the probability distribution of the position of the right-hand wall $X(t)$ for U and the constant value f $(= 1)$ with (a) $Y = 4.5$ under low temperature $(T = 0.1)$, (b) $Y = 4.5$ under high temperature $(T = 0.4)$, (c) $Y = 5.5$ under low temperature $(T = 0.1)$, and (d) $Y = 5.5$ under high temperature $(T = 0.4)$ conditions. Here, we set T with which the probability distribution of $X(t)$ has only one peak at $X(t) < 4$ (the solid-like state is realized) for the case of $U = 0$. The transition between the solid-like and liquid-like states with the temporal coexistence of the liquid-like and solid-like states is realized for $Y \leq 5.0$ by varying U [Figs. 3(a) and 3(b)]. In contrast with the case of $U = 0$ discussed previously, such a transition is observed also for the case with $Y > 5.0$. In these situations, the two particles are compressed near the top wall of the box by the asymmetric force with $U > 0$. This means that the region in which the particles spend almost all of

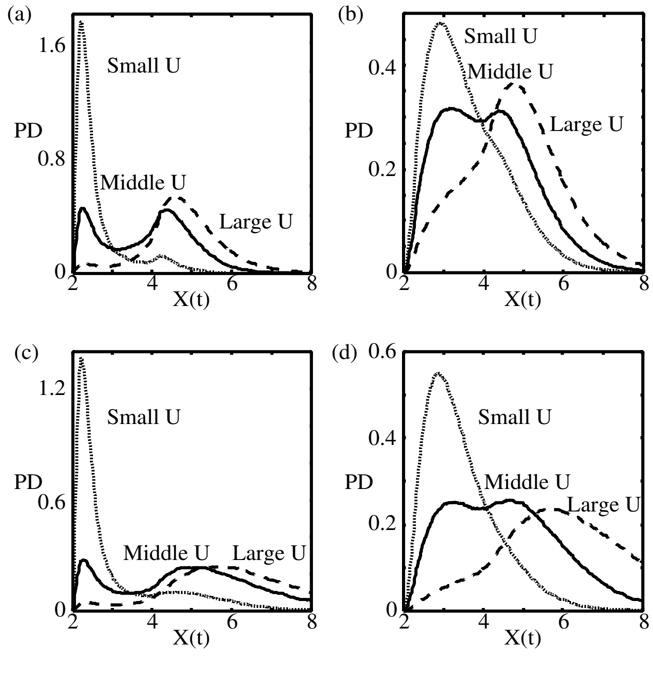

Fig. 3. Probability distribution of the position of the right-hand wall $X(t)$ (PD) for several values of U and $f = 1$ with (a) $Y = 4.5$ with $T = 0.1$ (middle $U = 1.14$), (b) $Y = 4.5$ with $T = 0.4$ (middle $U = 0.665$), (c) $Y = 5.5$ with $T = 0.1$ (middle $U = 1.925$), and (d) $Y = 5.5$ with $T = 0.4$ (middle $U = 1.25$).

their time becomes smaller along the vertical direction. Then, the Y-dependent characteristics of these transitions become blunt. With the increase of T and Y, these two peaks become smoother and the top of the probability distribution of $X(t)$ for mid-range U comes close to being flat [Fig. 3(d)].

Next, we focus on the characteristic features of frictions which emerge in the above system. We define the fluidity m of the system as the average frequency of the change of the sign of δy, where δy is the relative position between two particles in the vertical direction. The solid-like state is realized when $m \sim 0$, and the liquid-like state is realized when m is large. From the shear characterized by the velocity U, the force $F_{\rm ex} = \lim_{t\to\infty} \frac{1}{t}(\sum_{\rm col}(V_v - v_v))$ acts on particles at the left-hand wall in average. Here, $\sum_{\rm col}$ is the sum of individual collisions between the left-hand wall and particles. This value also gives the frictional force R between the particles and the left-hand wall. Figure 4 gives the relation between (a) U and m, and (b) U and R (or $F_{\rm ex}$) for several values of T for the constant values $f = 1$ and $Y = 5.0$. Here, the force f $(= 1)$ corresponds to the normal load of this system. Thus, in this case, the relations between U and R are equivalent to those between U and the effective friction coefficient $\mu = \frac{R}{f}$. For small U, $m \sim 0$ and $R \propto U$ are realized, while $m \propto U$ and $R = constant$ hold for large U. Here, the width of the box becomes larger as m becomes larger. Then, the frequency of collisions between a particle and the left-hand wall in contact with the energy source decreases. Hence, similarly to the dynamic friction of solid-on-solid systems which satisfy Coulomb–Amontons's friction laws,[1–3] R becomes almost constant for the increase of U when m becomes large. Moreover, R for each U becomes large with decreasing T. For small T, each U–R curve has one peak, and a marked change in R appears which is similar to the change between the static and dynamic frictions in the solid-on-solid system.[1–3] On the other hand, this peak disappears for large T. Figure 5(a) indicates the relations between m and R with increasing U for several values of T for the constant values $f = 1$ and $Y = 5.0$. In Fig. 5(a), for small T, R has a maximum value in the neighborhood of $m = 0$, and decreases monotonically and approaches a constant value with increasing m. These obtained profiles of m–R relations at $m \sim 0$ and large m are qualitatively similar to those of the velocity-friction relations of solid-on-solid systems.[1–3] For large T, R increases monotonically and becomes almost constant with increasing m, in contrast to the previous case. Next, we focus on the case with fixed U

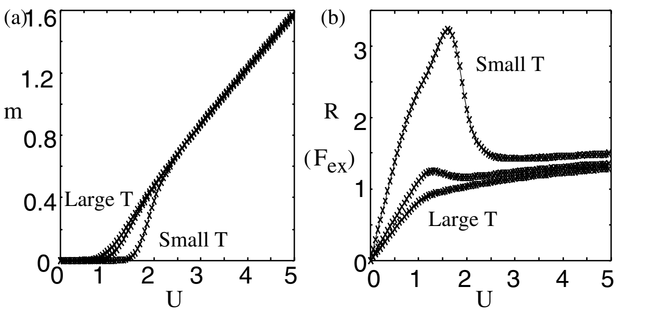

Fig. 4. Relations between (a) U and m and (b) U and R ($F_{\rm ex}$) for several values of T ($T = 0.06$, 0.24 and 0.42) with $Y = 5.0$ and $f = 1$.

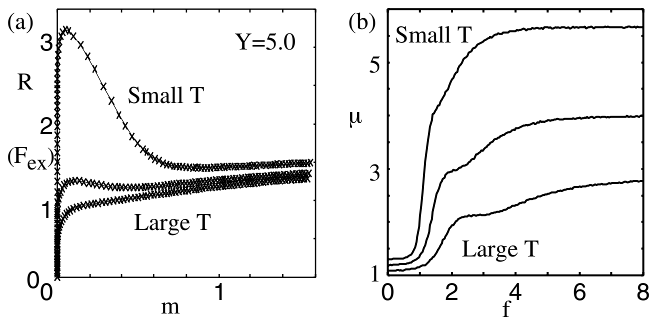

Fig. 5. (a) Relations between m and R ($F_{\rm ex}$) under the same condition as in Fig. 4. (b) Relations between f and μ for several values of T ($T = 2^{-5}$, 2^{-4} and 2^{-3}) for $Y = 5.0$ and constant U ($U = 2.0$).

and varying f. Figure 5(b) shows the relations between f and μ for several values of T for $U = 1$. In this case, the liquid-like state with large m and the solid-like state with $m \sim 0$ are realized for, respectively, small f and large f. In Fig. 5(b), μ has two plateau values at small f and at large f. This means that the frictional force R is almost proportional to the normal load f at small f and at large f like solid-on-solid frictions.[1–3] Moreover, μ of $m \sim 0$ states is larger than that of the large m states, and for mid-range f, μ for each T increases with increasing m. With the decrease of T, μ increases sharply. These properties were observed independent of Y.

We discuss the relation between the velocity of a plate on granular layers and the friction between the plate and the granular layers.[6–10] Through a recent and remarkable experiment, Nasuno *et al.* found that the relation between the plate velocity and the frictional force forms a hysteresis loop;[6,7] the frictional force is multi-valued, and is smaller for decreasing velocity to 0 than for increasing velocity from 0. It is interesting to note that the multi-valued frictional force is observed in the U-R relations in Fig. 4(b), in which R also depends on the temperature of the contacting heat bath. Therefore, we assume that U in Fig. 4(b) plays a similar role to the plate velocity, and R corresponds to the friction on granular layers. Based on the temperature dependency of R, we discuss a possible mechanism of history dependencies of velocity-friction relations on granular layers. Let us introduce a granular temperature $T_{\rm g}$ of the surface of granular layers as a half of the mean square of velocity fluctuation of each granular particle, and assume that $T_{\rm g}$ plays a role similar to the temperature of the energy source in our system. Initially, the plate and each particle in the granular layers do not move, and then $T_{\rm g} = 0$. Hence, immediately after the start of the slippage of the plate, $T_{\rm g}$ is expected to be small. As the plate movement becomes faster, however, $T_{\rm g}$ is expected to become larger because the plate excites particles in the granular layer. Then, considering the temperature dependency of R shown in Fig. 4(b), the frictional force immediately after the slippage is larger than that in the previous situation for the same slip velocity. Because of the friction, in the final stage, the plate stops and $T_{\rm g}$ becomes 0 again. In this granular system, $T_{\rm g}$ is expected to vary with time, which repeats as the plate is pushed continuously. This repetition and the temperature dependency of the frictional force explain the appearance of the hysteresis loop in the granular matter.

In this paper, we discussed the appearance and the change of frictions of a system with two particles in a box. First, in this simple system, we observed the liquid-like and solid-like states, and the transition between them. Next, we discussed the appearance of the frictional force of the system in which particles are excited by the shear in the vertical direction. In the simulation, we observed a marked change of the frictional forces similar to the change between the static and dynamic frictions observed in a solid-on-solid system. We found that the relation between the shear and the frictional forces strongly depends on the temperature of the heat bath. Taking these characteristics into consideration, we discussed the origin of the hysteresis loop in granular friction. Discovery of the temperature dependency of these characteristics of frictions is an important result of our simulation. Detailed numerical studies of the present problem are important for future work, as is analytical study of the dynamics of frictional forces on a granular layer.

The author is grateful to K. Kaneko, H. Nishimori, S. Sasa, K. Sato, K. Sekimoto, S. Nasuno, and S. Yukawa for useful discussions. This research was supported in part by Grant-in-Aid for JSPS Fellows 10376.

1) H. Matsukawa: Math. Sci. **433** (2000) 41 [in Japanese].
2) V. Zaloji, M. Urbakh and J. Klafter: Phys. Rev. Lett. **81** (1998) 1227.
3) E. Granato and S. C. Ying: Phys. Rev. Lett. **85** (2000) 5368.
4) M. O. Robbins and M. H. Müser: cond-mat/0001056 and references there in.
5) F. Heslot, T. Baumberger, B. Perrin, B. Caroli and C. Caroli: Phys. Rev. E **49** (1994) 4973.
6) S. Nasuno, A. Kudrolli and J. P. Gollub: Phys. Rev. Lett. **79** (1997) 949.
7) S. Nasuno, A. Kudrolli, A. Bak and J. P. Gollub: Phys. Rev. E. **58** (1998) 2161.
8) P. A. Thompson and G. S. Grest: Phys. Rev. Lett. **67** (1991) 1751.
9) J. M. Carlson and A. A. Batista: Phys. Rev. E **53** (1996) 4153.
10) H. Hayakawa: Phys. Rev. E **60** (1999) 4500.
11) A. Subbotin, A. Semenov and M. Doi: Phys. Rev. E **56** (1997) 623.
12) K. Sato and A. Toda: J. Phys. Soc. Jpn. **68** (1999) 77.
13) W. W. Wood and J. D. Jacobson: J. Chem. Phys. **27** (1957) 1207.
14) B. J. Alder and T. E. Wainwright: J. Chem. Phys. **27** (1957) 1208; *ibid.* **33** (1960) 1439.
15) W. G. Hoover and R. M. Ree: J. Chem. Phys. **49** (1968) 3609.
16) B. J. Alder and T. E. Wainwright: Phys. Rev. **127** (1962) 359.
17) J. A. Zollweg and G. V. Chester: Phys. Rev. B **46** (1992) 11186.
18) J. Lee and K. J. Strandburg: Phys. Rev. B **46** (1992) 11190.
19) J. P. Hansen and L. Verlet: Phys. Rev. **184** (1969) 151.
20) W. Vermhlen and N. Ito: Phys. Rev. E **51** (1995) 4325.
21) A. Awazu: Phys. Rev. E **63** (2001) 032102.
22) R. Tehver, F. Toigo, J. Koplik and J. R. Banavar: Phys. Rev. E **57** (1998) 65.